Selected for a Viewpoint in *Physics*
PRL **112,** 113004 (2014) PHYSICAL REVIEW LETTERS week ending 21 MARCH 2014

Direct Observation, Study, and Control of Molecular Superrotors

Aleksey Korobenko, Alexander A. Milner, and Valery Milner
Department of Physics and Astronomy, University of British Columbia, 6224 Agricultural Road, Vancouver, British Columbia, Canada V6T 1Z1

(Received 5 December 2013; published 19 March 2014)

Extremely fast rotating molecules whose rotational energy is comparable with the molecular bond strength are known as "superrotors." It has been speculated that superrotors may exhibit a number of unique properties, yet only indirect evidence of these molecular objects has been reported to date. Here we demonstrate the first direct observation of molecular superrotors by detecting coherent unidirectional molecular rotation with extreme frequencies exceeding 10 THz. The technique of an "optical centrifuge" is used to control the degree of rotational excitation in an ultrabroad range of rotational quantum numbers, reaching as high as $N = 95$ in oxygen and $N = 60$ in nitrogen. State-resolved detection enables us to determine the shape of the excited rotational wave packet and quantify the effect of centrifugal distortion on the rotational spectrum. Femtosecond time resolution reveals coherent rotational dynamics with increasing coherence times at higher angular momentum. We demonstrate that molecular superrotors can be created and observed in dense samples under normal conditions where the effects of ultrafast rotation on many-body interactions, intermolecular collisions, and chemical reactions can be readily explored.

DOI: 10.1103/PhysRevLett.112.113004 PACS numbers: 33.15.-e, 33.20.Sn, 33.20.Xx

Control of molecular rotation has been long recognized and successfully used as a powerful tool for steering chemical reactions in gases [1], and, at gas-surface interfaces [2,3], for imaging individual molecular orbitals [4] and generating extreme ultraviolet radiation [5,6], for deflecting molecular beams [7], and separating molecular isotopes [8]. The control is achieved by means of the spatial alignment of molecular axes and generally does not require a high degree of rotational excitation. On the other hand, extending the reach of rotational control to high rotational states is motivated by theoretical studies which show that ultrafast molecular rotation may change the character of molecular scattering from solid surfaces [9], alter molecular trajectories in external fields [10], increase stability against collisions [11], and lead to the formation of gas vortices [12]. New ways of molecular cooling [13] and selective chemical bond breaking [14] by ultrafast spinning have been suggested.

The appeal of rotational control has stimulated the development of multiple techniques in which molecules are exposed to strong nonresonant laser pulses [15,16]. However, bringing a large number of molecules to fast rotation is rather challenging. Conventional single-pulse excitation schemes lack selectivity with respect to the final speed of molecular rotation and produce broad rotational distributions [17]. Although sequences of pulses have been successfully used for selective [18–21] and directional [22–24] rotational excitation, the range of accessible rotational states has been limited to relatively low rotational quantum numbers (of order 10 above the initial state) due to the molecular breakdown in intense laser fields. To extend the range of accessible angular momenta, a number of theoretical proposals aimed at guiding the molecules up the "ladder" of rotational levels "step-by-step" instead of exerting a single ultrashort rotational kick [25–28]. An efficient method of accelerating molecular rotation with an "optical centrifuge" has been proposed [25] and successfully implemented [29–31]. Molecular spinning with an optical centrifuge, also realized in this work, is achieved by forcing the molecules to follow the rotating polarization of a laser field. The final speed of rotation is determined by the spectral bandwidth of the laser pulse and may exceed 10^{13} Hz. To make O_2 molecules rotate primarily with this speed in thermal equilibrium, the gas temperature would have to have risen to above 50 000 Kelvin.

Since the original proposal [25], an optical centrifuge has been implemented by two experimental groups. In the pioneering work by Villeneuve *et al.*, dissociation of chlorine molecules exposed to the centrifuge field has been attributed to the breaking of the Cl-Cl bond which could not withstand the extremely high spinning rates [29]. More recently, Yuan *et al.* observed rotational and translational heating in the ensembles of CO_2 and N_2O molecules and associated it with the collisional relaxation of the centrifuged species [30,31]. In both cases, an *incoherent* secondary process (i.e., dissociation and multiple collisions) has been used for indirect identification of the formation of super rotors whose most unique property—their synchronous unidirectional rotation, remained hidden. In this work, we employ a *coherent* detection technique, which enables direct detection of molecular super rotors with high frequency and time resolution. We follow the molecules as they spin-up inside the rotating laser field and, after releasing them from the centrifuge, examine the influence of ultrafast rotation on their rotational dynamics.

To produce both the centrifuge and probe pulses we start with the output of a regenerative Ti:sapphire amplifier which generates femtosecond pulses of 30 nm spectral bandwidth [full width at half maximum (FWHM)] centered around 792 nm. Following the recipe of Karczmarek *et al.* [25], we create an optical centrifuge [Fig. 1(a)] by splitting an ultrashort laser pulse at the center of its spectrum [horizontal dashed line in Figs. 1(b),(c)] with a home built pulse shaper. The shaper is used to apply an opposite frequency chirp to the two spectral halves of the pulse, as shown by the time-frequency spectrogram in Fig. 1(c). The two spectral components are combined on a polarizing beam splitter cube and polarized with an opposite sense of circular polarization by means of a quarter-wave plate. Their interference results in a rotating linearly polarized field of the centrifuge. The instantaneous frequency difference, $2\Omega(t)$, between the left and right circularly polarized components grows in time, resulting in a gradual increase of the centrifuge angular frequency $\Omega(t)$.

To terminate the acceleration and release of the molecules with a well-defined final angular frequency, the spectrum of the centrifuge pulse is truncated symmetrically around the central wavelength, as shown in Fig. 1(b). After the second stage of amplification, carried out with a home built Ti:sapphire multipass amplifier, the total energy of the centrifuge is ≈50 mJ/pulse at 10 Hz repetition rate. Characterization of the centrifuge field [Fig. 1(c)] shows that its angular frequency gradually increases from 0 to 10 THz in the course of about 70 ps.

Key to this work is the use of coherent Raman scattering of probe light from the rotating molecules. Quantum mechanically, synchronous molecular rotation corresponds to a superposition of a few rotational quantum states—a “rotational wave packet,” with an average frequency separation matching the frequency of the classical rotation. Owing to the time-dependent wave packet coherence between the quantum states separated by $\Delta N = \pm 2$, the probe spectrum acquires a frequency sideband shifted down or up from the central probe frequency, depending on whether the molecules rotate in the same or opposite direction with respect to the probe polarization. In both cases, illustrated in Fig. 1(d), the magnitude of the Raman shift equals twice the rotation frequency, while its sign reflects the direction of molecular rotation. In classical terms, the frequency shift can also be viewed as a result of the rotational Doppler effect [32].

The probe beam is spectrally narrowed to either ≈0.1 or ≈0.4 nm FWHM (for frequency- and time-resolved detection, respectively) with a separate pulse shaper, and then frequency doubled to produce pulses centered around 396 nm with a total energy of $< 1\ \mu\mathrm{J/pulse}$. As shown in Fig. 1(e), the two beams are combined on a dichroic beam splitter and focused with a single 1000 mm lens to a focal beam waist of ≈120 μm FWHM into a windowless cell containing oxygen or nitrogen at room temperature and atmospheric pressure. Loose focusing is used to avoid ionization and plasma breakdown by limiting the peak intensity of the excitation field to below $5 \times 10^{12}\ \mathrm{W/cm^2}$. Probe pulses, polarized with a circular polarizer and

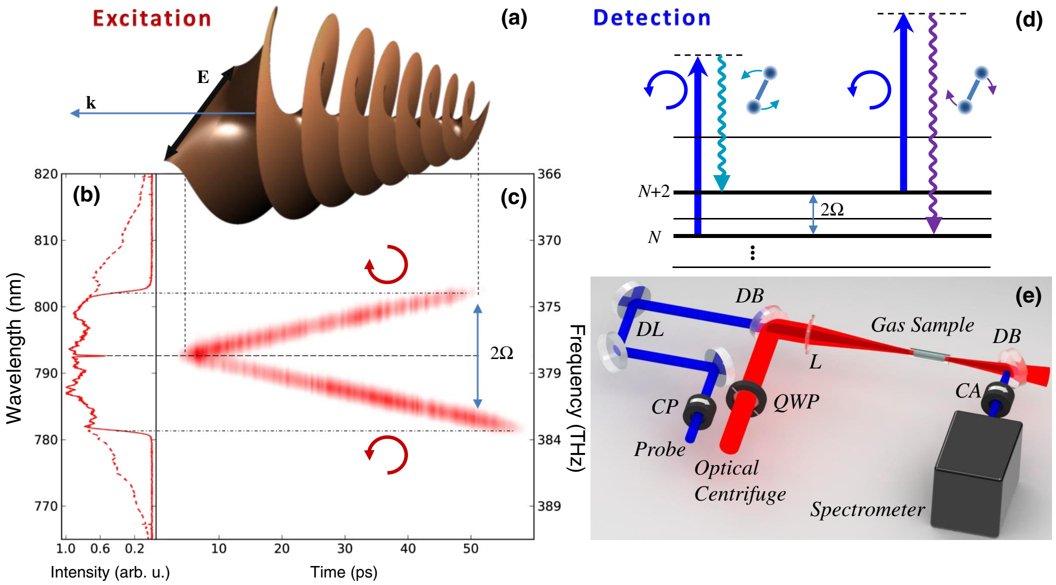

FIG. 1 (color online). (a) Illustration of an optical centrifuge field propagating in the direction **k**. The vector of linear polarization **E** undergoes an accelerated rotation. (b) Frequency spectra of a full (dashed) and truncated (solid) centrifuge pulse. (c) Time-frequency spectrogram of the centrifuge field, recorded by means of cross-correlation frequency resolved optical gating. (d) The speed and direction of molecular rotation is detected by measuring the magnitude and sign of coherent Raman scattering, respectively. (e) Experimental setup. Circular polarizer (CP), circular analyzer (CA), dichroic beam splitter (DB), delay line (DL), quarter-wave plate (QWP).

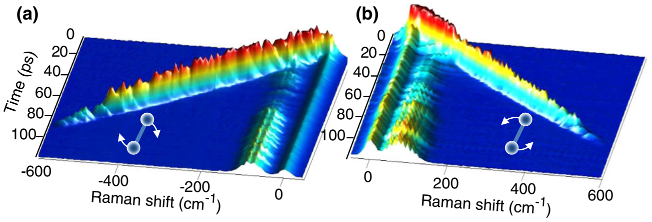

FIG. 2 (color online). Time-dependent Raman shifts from the clockwise (a) and counterclockwise (b) centrifuged oxygen molecules. As the molecules spend a longer time in the centrifuge, the observed Raman frequency shift increases, providing direct evidence of accelerated molecular rotation in one well defined direction. An additional time-independent Raman signal originates from the molecules lost from the centrifuge.

delayed with a delay line, are scattered off the centrifuged molecules. After the output stage of polarization and wavelength filtering, the probe spectrum is recorded with a 0.1 nm-resolution spectrometer.

Delaying the arrival time of probe pulses with respect to the beginning of the centrifuge pulse enables us to observe the spinning molecules before and after they leave the centrifuge. In Figs. 2(a) and 2(b), the rotational Raman spectrum of oxygen is plotted as a function of the time the molecules spent in the centrifuge. The growing frequency shift of the Raman sideband indicates the expected increase of the laser-induced spinning rate. The two plots correspond to two opposite senses of the centrifuge rotation and demonstrate the direct evidence of molecular spinning in a well-defined direction.

To identify the excited rotational levels, we narrow the probe bandwidth down to7.5 cm^{-1} (FWHM) and analyze the spectrum of the Raman signal. The results, corresponding to different centrifuge durations and, therefore, different degrees of rotational excitation, are shown in Fig. 3(a) for the case of O_2. Each measured spectrum consists of three parts: (i) an unshifted probe line at 0 cm^{-1}; (ii) a set of stationary lines centered around 80 cm^{-1} and corresponding to the molecules lost from the centrifuge during its spinning; and (iii) a set of moving lines corresponding to the molecules which followed the centrifuge up to its terminal angular frequency.

Well-resolved peaks in the spectrum correspond to the individual Raman transitions between the states with rotational quantum numbers $N-2$ and N. The group of the Raman-shifted lines on the right side of the spectra in Fig. 3(a) reflects an accelerated rotation of the molecules trapped in the centrifuge field, and demonstrates our ability to control the degree of rotational excitation. Quantum numbers N can be easily assigned by counting the peaks. Only odd values of N are allowed for the $^{16}O_2$ molecule because of its nuclear spin statistics.

In a rigid rotor approximation, the rotational energy is $E(N) = BN(N+1)$, where B is the rotational constant of the molecule. This scaling results in a series of equidistant Raman peaks separated by $\Delta\Omega = 4B\Delta N$, with ΔN being the smallest possible step in the molecular rotational ladder (e.g., 1 for N_2 and 2 for O_2). However, as one can see in Fig. 3(b), the measured peak separation does not stay constant, but rather decreases with increasing angular momentum—a direct consequence of the centrifugal distortion evident at $N > 50$. Being able to resolve the energies of extreme rotational states, we quantify the magnitude of the centrifugal distortion and verify that it is well described by the Dunham expansion to second power in $N(N+1)$ [green solid lines in Fig. 3(b)].

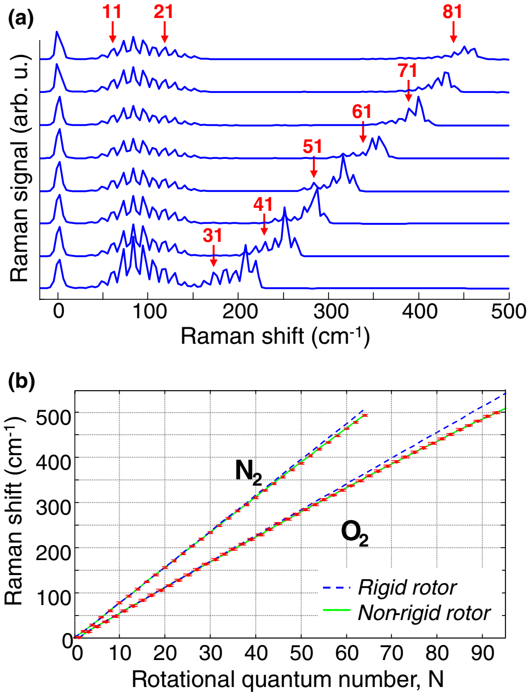

FIG. 3 (color online). (a) State-resolved Raman spectra of the centrifuged oxygen molecules. Higher curves correspond to longer spinning time inside the centrifuge. Red vertical arrows mark the rotational quantum numbers. (b) Experimental (dots with error bars) and calculated (dashed blue and solid green for the rigid and nonrigid rotor approximations, respectively) rotational energy spectrum expressed as a Raman frequency shift.

To study the rotational motion of the superrotors, we shorten the length of the probe pulses to 500 fs and examine the time dependence of the Raman response. As shown by a tilted trace in Fig. 4(a), the rotation of molecules trapped in the centrifuge follows the angular frequency of the laser field. A horizontal trace at the end (beginning) of the centrifuge pulse at $N \approx 79$ ($N \approx 15$) indicates the free rotation of molecular super rotors, released (lost) from the centrifuge. The observed oscillatory signal, emphasized in the inset, is indicative of coherent rotational dynamics. In agreement with the general theory of quantum wave packets [33,34], the evolution of freely rotating molecules exhibits a discrete set of commensurate periods, revealed

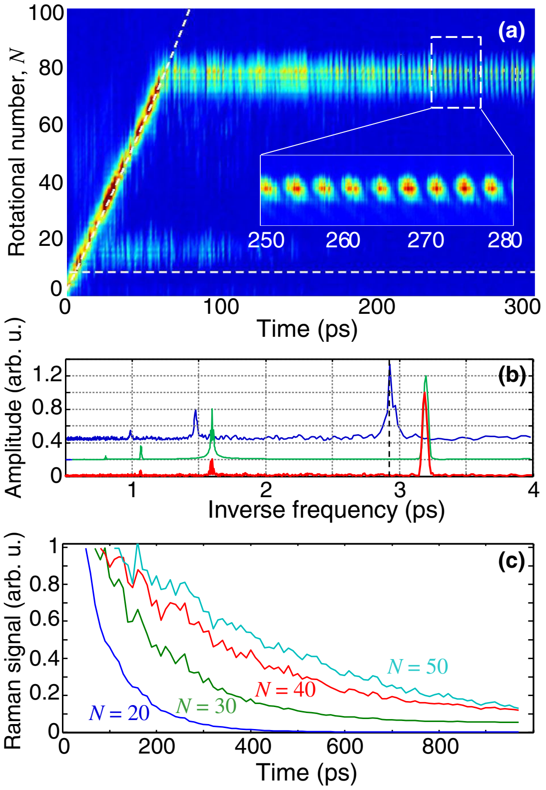

FIG. 4 (color online). (a) Scattered light intensity as a function of time and frequency, converted to the rotational quantum number of oxygen. Dashed tilted line shows the increasing angular frequency of the centrifuge, terminated at about 70 ps. Dashed horizontal line marks the most populated rotational state of O_2 at room temperature, $N = 9$. Oscillations of the coherent rotational wave packet are shown in the inset, whereas their Fourier transform is plotted in panel (b) as a function of the inverse frequency. Lower red and middle green curves represent our experimental data and numerical simulations, respectively. The upper blue curve shows the experimental results for a weaker rotational excitation around $N = 29$, and the vertical dashed line indicates the anticipated oscillation period of a rigid rotor. (c) State-resolved decay of rotational coherence in nitrogen.

by a Fourier transform of the collected data [Fig. 4(b)]. In the case of oxygen at $N \approx 79$, the initial period of 1.6 ps changes to twice that value at later times. The periods are inversely proportional to the second derivative of $E(N)$ with respect to N, i.e., $T = \{8Bc[1 - 6\epsilon N(N+1)]\}^{-1}$, where c is the speed of light in vacuum and $\epsilon := D/B \approx 3 \times 10^{-6}$ is the ratio between the two rotational constants in the Dunham expansion. For a rigid-rotor model ($\epsilon = 0$) of oxygen, this would result in the main period of $T = (8Bc)^{-1} \approx 2.9$ ps, marked by a vertical dashed line in Fig. 4(b) and in agreement with our results for "slow" rotation ($N = 29$, upper blue curve). Centrifugal distortion of fast superrotors ($N = 79$) results in the stretching of the molecular bond and the correspondingly longer rotational period, as illustrated by the experimental results (bottom red line) and numerical calculations (middle green line) in Fig. 4(b). Note that breaking the oxygen bond would require a much higher $N \approx 250$.

The combination of frequency and time-resolved detection enables us to study the decay of rotational coherence at various levels of excitation. Figure 4(c) shows the observed increase of rotational stability with increasing N in nitrogen super rotors. Given the average time of 138 ps between the collisions of N_2 at room temperature and atmospheric pressure, this observation suggests that a single collision is sufficient to scramble the phase of a slow molecular rotor, while more collisions are needed to de-phase an ensemble of fast super rotors. Our results extend the previous work on rotational decoherence at low angular frequencies ($N \approx 15$ in nitrogen [35]) and point to the qualitative difference between the collisions of fast and slow rotating molecules. At $N = 50$, the rotational period of N_2 is about 168 fs, more than 3 times shorter than the characteristic collision time of 560 fs, estimated as the ratio of the molecule's "hard sphere diameter" and its thermal velocity. At this limit, angular averaging may result in a smaller perturbation to the rotational phase in comparison with that of a slower rotator (e.g., $N = 20$) for which the rotational period (419 fs) approaches the collision time scale [36].

Direct observation and versatile control of molecular rotation in an extremely broad range of angular frequencies reported in this work paves the way for exploring novel science with molecular superrotors. Studies of electrical, optical, and magnetic properties of these exotic objects are underway and promise to offer interesting possibilities in controlling molecular dynamics.

This work has been supported by the CFI, BCKDF, and NSERC. We thank Gilad Hurvitz and Sergey Zhdanovich for their help with the experimental setup. We gratefully acknowledge stimulating discussions with John Hepburn, Ilya Averbukh, Yehiam Prior, and Ed Grant.

[1] R. N. Zare, Science **279**, 1875 (1998).
[2] E. W. Kuipers, M. G. Tenner, A. W. Kleyn, and S. Stolte, Nature (London) **334**, 420 (1988).
[3] D. Shreenivas, A. Lee, N. Walter, D. Sampayo, S. Bennett, and T. Seideman, J. Phys. Chem. A **114**, 5674 (2010).
[4] J. Itatani, J. Levesque, D. Zeidler, H. Niikura, H. Pepin, J. C. Kieffer, P. B. Corkum, and D. M. Villeneuve, Nature (London) **432**, 867 (2004).
[5] J. Itatani, D. Zeidler, J. Levesque, M. Spanner, D. M. Villeneuve, and P. B. Corkum, Phys. Rev. Lett. **94**, 123902 (2005).
[6] N. Wagner, X. Zhou, R. Lock, W. Li, A. Wüest, M. Murnane, and H. Kapteyn, Phys. Rev. A **76**, 061403 (2007).
[7] S. M. Purcell and P. F. Barker, Phys. Rev. Lett. **103**, 153001 (2009).
[8] S. Fleischer, I. Sh. Averbukh, and Y. Prior, Phys. Rev. A **74**, 041403 (2006).
[9] Y. Khodorkovsky, J. R. Manson, and I. Sh. Averbukh, Phys. Rev. A **84**, 053420 (2011).

[10] E. Gershnabel and I. Sh. Averbukh, Phys. Rev. Lett. **104**, 153001 (2010).
[11] K. Tilford, M. Hoster, P. M. Florian, and R. C. Forrey, Phys. Rev. A **69**, 052705 (2004).
[12] U. Steinitz, Y. Prior, and I. Sh. Averbukh, Phys. Rev. Lett. **109**, 033001 (2012).
[13] R. C. Forrey, Phys. Rev. A **66**, 023411 (2002).
[14] R. Hasbani, B. Ostojic, P. R. Bunker, and M. Y. Ivanov, J. Chem. Phys. **116**, 10636 (2002).
[15] B. Friedrich and D. Herschbach, Phys. Rev. Lett. **74**, 4623 (1995).
[16] H. Stapelfeldt and T. Seideman, Rev. Mod. Phys. **75**, 543 (2003).
[17] T. Seideman, J. Chem. Phys. **115**, 5965 (2001).
[18] M. Renard, E. Hertz, B. Lavorel, and O. Faucher, Phys. Rev. A **69**, 043401 (2004).
[19] S. Fleischer, I. Sh. Averbukh, and Y. Prior, Phys. Rev. Lett. **99**, 093002 (2007).
[20] J. P. Cryan, P. H. Bucksbaum, and R. N. Coffee, Phys. Rev. A **80**, 063412 (2009).
[21] S. Zhdanovich, C. Bloomquist, J. Floss, I. Sh. Averbukh, J. W. Hepburn, and V. Milner, Phys. Rev. Lett. **109**, 043003 (2012).
[22] S. Fleischer, Y. Khodorkovsky, Y. Prior, and I. Sh. Averbukh, New J. Phys. **11**, 105039 (2009).
[23] K. Kitano, H. Hasegawa, and Y. Ohshima, Phys. Rev. Lett. **103**, 223002 (2009).
[24] S. Zhdanovich, A. A. Milner, C. Bloomquist, J. Floss, I. Sh. Averbukh, J. W. Hepburn, and V. Milner, Phys. Rev. Lett. **107**, 243004 (2011).
[25] J. Karczmarek, J. Wright, P. Corkum, and M. Ivanov, Phys. Rev. Lett. **82**, 3420 (1999).
[26] J. Li, J. T. Bahns, and W. C. Stwalley, J. Chem. Phys. **112**, 6255 (2000).
[27] N. V. Vitanov and B. Girard, Phys. Rev. A **69**, 033409 (2004).
[28] J. P. Cryan, J. M. Glownia, D. W. Broege, Y. Ma, and P. H. Bucksbaum, Phys. Rev. X **1**, 011002 (2011).
[29] D. M. Villeneuve, S. A. Aseyev, P. Dietrich, M. Spanner, M. Y. Ivanov, and P. B. Corkum, Phys. Rev. Lett. **85**, 542 (2000).
[30] L. Yuan, S. W. Teitelbaum, A. Robinson, and A. S. Mullin, Proc. Natl. Acad. Sci. U.S.A. **108**, 6872 (2011).
[31] L. Yuan, C. Toro, M. Bell, and A. S. Mullin, Faraday Discuss. **150**, 101 (2011).
[32] O. Korech, U. Steinitz, R. J. Gordon, I. Sh. Averbukh, and Y. Prior, Nat. Photonics **7**, 711 (2013).
[33] C. Leichtle, I. Sh. Averbukh, and W. P. Schleich, Phys. Rev. Lett. **77**, 3999 (1996).
[34] T. Seideman, Phys. Rev. Lett. **83**, 4971 (1999).
[35] M. L. Koszykowski, L. A. Rahn, R. E. Palmer, and M. E. Coltrin, J. Phys. Chem. **91**, 41 (1987).
[36] A. Korobenko, A. A. Milner, J. W. Hepburn, and V. Milner, (to be published).